Vol. 17(1), pp. 10-22, January-March, 2022
DOI: 10.5897/IJPS2021.4974
Article Number: 321FAFB68562
ISSN 1992-1950

http://www.academicjournals.org/IJPS

ACADEMIC JOURNALS

International Journal of Physical Sciences

Full Length Research Paper

Mantle electrical conductivity determination employing the ionospheric solar quiet day (Sq) currents in the Southern African regions

Ngozi Agatha Okwesili[1*], Francisca Nneka Okeke[1], Daniel Nnaemeka Obiora[1], John Akor Yakubu[1], Johnson Uchenna Abangwu[1] and Kiyohumi Yumoto[2]

[1]Department of Physics and Astronomy, University of Nigeria, Nsukka, Enugu State, Nigeria.
[2]Space Environment Research Centre, Kyushu University, Fukuoka, Japan.

Received 30 October, 2021; Accepted 8 December, 2021

Solar quiet (Sq) daily currents variation obtained in the Hermanus (34.34°S, 19.22°E), Tsumeb (19.24°S, 17.72°E), Hartebeesthoek (25.68°S, 28.09°E) and Maputo (25.97°S, 32.57°E), were employed in determining the mantle electrical conductivity depth profile of the Southern African region. The external and internal contributions in the solar quiet field were separated using the spherical harmonic analysis (SHA), after which, the transfer functions were used to compute the electrical conductivity depth profiles of the region. A downward increase was observed in electrical conductivities and deep depth of penetration within the Earth regions. In Hartebeesthoek, Hermanus, Maputo and Tsumeb, the evaluated average electrical conductivity values are 0.028 Sm^{-1}, 0.039 Sm^{-1}, 0.057 Sm^{-1} and 0.0.025 Sm^{-1} at depths of 76.4 km, 84.1 km,141.0 km and 111.5 km at the respective maximum depths of penetration of 1052.8 km, 1467.0 km, 1160.8 km and 1289.5 km in Hartebeesthoek, Hermanus, Maputo and Tsumeb, the calculated electrical conductivity reached the maximum values of 0.498 Sm^{-1}, 0.323 Sm^{-1}, 0.387 Sm^{-1} and 0.187 Sm^{-1} respectively. Discontinuities were observed in all the profiles but are more prominent in Tsumeb region near 390.0 - 750.0 km, 820.0 - 980.0 km and 200.0 - 300.0 km. From these results, we are stating that the effects from the deeper 3-D structures (such as gold, copper etc), the hydrated transition zone and effect from the ocean contribute to the greater depth of Sq penetration.

Key words: Solar quiet currents, Southern Africa, electrical conductivity, spherical harmonic analysis, Mantle.

INTRODUCTION

Geomagnetism is a science that is intimately connected with the physics of the upper atmosphere as well as the rather varies with time partly due to the solar wind interaction, and more importantly by its own physical processes (Kono, 2009). The Earth's magnetic fields are caused mostly by influences from solar variability and solar activity on ionosphere and magnetosphere. These fluctuating external fields induce electric currents into the Earth, which in turn, depending on the conductivity of the subsurface regions produce changing induced magnetic

*Corresponding author. Email: ngozi.okwesili@unn.edu.ng.

fields. Other types of secondary induced fields which vary at short times are being produced within the oceans. Also, secondary magnetic fields are generated through the process of magneto-hydrodynamic motional induction by the movement of the electrically conducting sea water in the geomagnetic field (Glaßmeier et al., 2009).

The geomagnetic fields measured at the surface of the Earth or on board the satellites results from the sum of several field contributions from different sources with different physical origins. These sources can be found both above the Earth's surface (in the form of electrical currents) and below (in the form of magnetized materials and electrical currents). Each of these sources produces a contribution with rather specific spatiotemporal characteristics. These are external contribution which originate from the currents in the magnetosphere and ionosphere as well as the internal contributions like the main field, also called the core field, and the lithospheric or crustal field. The main field occurs due to the electrical currents in the outer core of the Earth at depths greater than 2,900 km with its strength varying from less than 30,000 nT near the equator to about 60,000 nT near the poles, making the main field responsible for more than 95% of the field observed at the (Olsen, 1999). Magnetized materials in the crust cause the lithospheric field which is relatively weak and accounts for only but a few percent of the field observed at ground. External magnetic field contributions are also on the average, relatively weak- a few percent of the total field at ground during geomagnetic field quiet conditions. But, if not checked properly, they will disturb the precise determination of the internal field. Therefore it is very important to account for the external field contribution (by data selection, data correction, and/or field co-estimation) to obtain a reliable model of the internal fields (Ugbor et al., 2016).

Hellibrand in 1634 at London gave the first reports of a regular quiet-day variation of the geomagnetic field from the careful observations of the motion made by the end point of the long magnetic compass needle (Von Humboldt, 1863). This quiet variation was also later discovered independently by Tachard (1685). But, this variation was not truly accepted until Graham (1724) made his first calibrated routine determinations of quiet variations in the declination, Sq (D) and he first observed the Sq variation of the geomagnetic field. Also, Canton (1759), towards the latter part of 18th Century discovered the seasonal variability of the Sq field by noting that the quiet day variations (Sq) are greater in summer than in winter. Measurements made by Canton (1759) and by Cassini, Beaufoy, Gilpin, Celcius and Hiorter (Von Humboldt, 1863) had established that the seasonal variation of the diurnal fluctuation amplitudes was more than a local phenomenon. Subsequently, Sabine (1846) determined the lunar and Sq field variations at his observatories and also discovered that the magnetic field intensities varied in parallel with the changes in the sunspot. Gauss (1839) proved that, the magnetic field of a region of free electric currents can be represented by a scalar function, called potential function. For practical purposes, the space near the earth is current-free; therefore Gauss' result applies, so he derived a model potential function, using a spherical harmonic expansion. Since years, spherical harmonic expansion is taken to be the usual form of such models, even though occasionally a different form is chosen. A geomagnetic field model is then, a potential function which represents the measured field, often in a best least-square sense. These models mostly represent only the fields originating within the earth and only the portion of that internal field originate in the core (Langel, 1982). The main, or core field is actually the major portion of the measured field and its magnitude at the Magsat altitude is between 30,000 and 60,000 nanoteslas. Crustal source fields, ranges from 0 to 50 nanoteslas and external source fields are generally between 0 and 1000 nanoteslas, hence accurate main-field models are crucial to the study of other source fields (Langel, 1982).

Furthermore, Schuster (1889, 1908) made an innovation to Gauss' spherical harmonic analysis (SHA) method by adapting it to the measurements of geomagnetic field daily variations, representing the observations using few harmonic terms. He discovered that the internal/external ratio of the geomagnetic potential was just about 4, thereby proving that the Sq source is external to the earth. Meanwhile, Schmucker (1970) established the transfer function equations which are necessary in obtaining conductivity-depth profile from the separated internal and external SHA fields. This was followed by a subsequent series of publications which extended the Schmucker work with conductivity analyses of continental half-sectors (Arora et al., 1995; Campbell, 1987, 1997; Campbell and Schiffmacher, 1986, 1988, 1988b; Campbell and Anderssen, 1983). Thus, by the turn of the century, it was proven that the quiet-time geomagnetic field daily variations came from sources of current mostly external to the Earth through the spherical harmonic analysis application (Schuster, 1889, 1908). Since then, many researchers have worked on the solar quiet (Sq) day variations but not much work has been done on applying this Sq variation to study the interior of the Earth. Although Sq was applied to map out conductivity–depth structure of the upper mantle in West Africa and East Africa, not much was done in Southern African regions especially Maputo and Hartebeesthoek regions were no work has been done at all. Therefore, together with the works of other researchers who worked in different regions of Africa, we hope to consolidate our knowledge of the internal structure, composition and physical state of the African plate in general as we incorporate the striking features of the upper atmosphere and that of the Earth’s interior.

However, Chapman and Price (1930), and Chapman (1919) started the earlier works done on the use of Sq

variation in determining the electrical conductivity depth profiles of the mantle when they utilized the separated internal and external fields' contributions to determine the conductivity depth structure of the Earth. Presently, the application of the Sq in probing the electrical conductivity depth profile of the interior of the Earth is attracting more researchers' attention. For example, Campbell and Anderssen (1983) performed a research work on the electrical conductivity of the sub continental upper mantle: using quiet-daily geomagnetic records observed in North America. Also, Campbell and Schiffmacher (1986) did a comparative study of the upper mantle sub continental conductivity of Asia, Europe and North America. Campbell et al. (1998) and Arora et al. (1995) also established the conductivity-depth structure of Australian and Himalayan regions respectively. Furthermore, Agha and Okeke (2007) using Sq variation estimated the conductivity-depth ratio of various sub-regions of the upper mantle in L' Aquila. Obiora et al. (2013) and Obiekezie and Okeke (2010) similarly reported the conductivity-depth profiles in West Africa. Ugbor et al. (2016) used solar quiet (Sq) daily variations in determining mantle conductivity depth profile of the African geomagnetic equatorial zones. Abidin et al. (2019) determined the mantle conductivity depth profile of Malaysia employing solar quiet (Sq) daily current variations. Hence in this research work, we studied extensively the upper mantle conductivity-depth structure within the Southern African region using the application of Sq current variations and compared our result with the works of Obiora and Okeke (2013) done in west Africa and Campbell and Schiffmacher (1988) done in Australia.

MATERIALS AND METHODS

Sources of data

The fields data used in the work are one minute and one hour geomagnetic (H, D and Z) field's data sets of four Southern African regions. The Hermanus (latitude 34.34°S, longitude 19.22°E), Tsumeb (latitude 19.24°S, longitude 17.72°E) and Hartebeesthoek (latitude 25.68°S, longitude 28.09°E) one hour field data were obtained from World Data Center, WDC for Geomagnetism, Kyoto Japan. Additionally, Maputo (latitude 25.97°S, longitude 32.57°E), one minute field data was obtained from magnetometer installed by the Magnetic Data Acquisition System (MAGDAS) and courtesy of the Space Environment Research Center, Kyushu Japan. The international geomagnetic quiet day (IQD) for the year understudy was also obtained from Geoscience Australia and World Data Center (WDC) Kyoto, Japan website. The data used was acquired in 2011.

Data analysis

For the application of solar quiet ((Sq) daily current variation to conductivity modeling, the size of the geomagnetic field current sources must be large in respect to the skin depth of the region to be probed. Also, the current source must be well behaved; meaning that it must change only slowly and smoothly, in linearly prescribed ways. Therefore, the solar quiet (Sq) daily current variations gotten from the field records of geomagnetic observatories meet this requirement for determining the upper mantle conductivity of the Earth (Campbell, 2003). Maxwell (1873) started the solar quiet (Sq) daily current variations application into the Earth's interior with the formulation of the electromagnetic differential field's equations. He assumed in one of his adjusted equations that only negligible electric field variations occur and that there is relatively an insignificant amount of current flowing across the boundary between the atmosphere and the earth. Hence at the surface of the earth, the potential function V for the earth's main field (devised by Gauss in 1838) which satisfies this requirement has the converging series of terms as (Campbell, 2003):

$$V = a\sum_{n=1}^{\infty}\left[\left(\frac{r}{a}\right)^{n} S_n^{e} + \left(\frac{a}{r}\right)^{n+1} S_n^{i}\right] \tag{1}$$

Where the Earth radius (R_e), is a while $e\ and\ i$ superscripts means external and internal respectively. There are two series for V . First is the r^n terms series and second is the $\left(\frac{1}{r}\right)^n$ terms series. For the first series, as r is increasing, these terms become increasingly larger; meaning that one is moving away from the earth and therefore must be approaching the external field source current. In the second series, as r is becoming smaller and smaller, these terms become larger and larger meaning that we are moving down into the earth and must be approaching the source current of an internal field. In geophysical problems such as solar quiet (Sq) analysis, this series represent the separation of the geomagnetic potential function of the earth into its internal (induced) and external (ionosphere source) contributions of the geomagnetic field. This process allows for the construction of the ionosphere dynamo-current systems, and the induced fields also give information on the earth's electrical conductivity profile. Therefore, the general expression for the magnetic potential function of the solar quiet (Sq) field V measured from the daily average values at universal time T written as a sum of spherical harmonies for both the external and internal current sources is given by Gauss (1838) as where $c, \theta, a, r, and\ \emptyset$ is the integration constant, the geomagnetic colatitudes, the earth's radius, the geocentric distance and the local

$$V_n^{\ m} = C + a\sum_{n=1}^{\infty}\sum_{m=0}^{n}\left[\left\{a_n^{me}\left(\frac{r}{a}\right)^{n} + a_n^{mi}\left(\frac{a}{r}\right)^{n+1}\right\}\cos(m\phi) + \left\{b_n^{me}\left(\frac{r}{a}\right)^{n} + b_n^{mi}\left(\frac{a}{r}\right)^{n+1}\right\}\sin(m\phi)\right]p_n^{m}(\theta) \tag{2}$$

time of the observatory respectively. The $a_n^{me} and\ a_n^{mi}, b_n^{me}\ and\ b_n^{mi}$ are Legendre polynomial (Schmidt) coefficients where $e\ and\ i$ show the external and internal values respectively. The p_n^m are Legendre polynomial (Schmidt) functions of colatitudes θ only, where as the integers $m\ and\ n$ are called order and degree respectively; m is always less than or equal to n and n has a value of 1 or greater. The Legendre polynomial (Schmidt) functions p_n^m are computed as (Campbell, 1997):

$$R_n^m = \sqrt{n^2 - m^2};\ P_0^0 = 1;\ P_1^0 = \cos(\theta);\ P_1^1 = \sin(\theta) \tag{3}$$

$$P_m^m = \sqrt{\frac{2m-1}{2m}}\sin(\theta)P_{m-1}^{m-1} \qquad for\ m > 1,\ n = m \tag{4}$$

$$P_n^m = \frac{[(2n-1)\cos(\theta)P_{n-1}^m - R_{n-1}^m P_{n-2}^m]}{R_n^m} \qquad for\ n > m \tag{5}$$

$$\frac{dP_n^m}{d\theta} = \frac{(n\cos(\theta)P_n^m - R_n^m P_{n-1}^m)}{\sin(\theta)} \quad (except\ for\ \theta = 0°\ or\ 180°) \tag{6}$$

At the poles, Equation 6 is undefined ($\theta = 0°\ or\ 180°$).

For Sq analysis, the radius of the Earth, a, is approximately taken to be equal to geocentric distance, r ($r \approx a$).

Using $\left(a_n^{me} + a_n^{mi}\right) = A_n^m\ and\ \left(b_n^{me} + b_n^{mi}\right) = B_n^m$,

Equation 2 then becomes

$$V_n^m(\theta, \emptyset) = R_e \sum_{n=1}^{\infty} \sum_{m=0}^{n} [A_n^m \cos(m\emptyset) + B_m \sin(m\emptyset)]\, P_n^m(\theta) \tag{7}$$

From the geomagnetic field potential functions solution (Equation 7), the functions that are multiplying the Legendre polynomial terms appear like a Fourier series which is a harmonic series of cosine and sine terms that, when added, produces the function they are to represent. In Fourier analysis, there is an assumption that the wave form being fitted repeats in every interval for both directions outside the region of interest. Therefore, when studying some values along a latitude line of a sphere, the fitted waves repeat by the natural closing around the circle of fixed latitude.

In spherical harmonic analysis, for the function being fit to the data (Equation 7), the A_n^m and B_n^m are amplitude coefficients, the $\cos(m\emptyset)$ and $\sin(m\emptyset)$ are sinusoidal oscillations about a latitude circle, and the $P_n^m(\theta)$ are the Legendre wave oscillations along a great circle of longitude. Hence, to implement Gauss coefficients of the SHA when what we have are the measurements of $X,\ Y, and\ Z$ fields about the earth, first of all, some extrapolation and smoothing arrangement are followed so that the three – component field observations are represented at evenly spaced latitude and longitude locations all over the entire earth. Next, at each colatitude θ, a Fourier analysis done along the latitude line provides m sine and cosine coefficients to represent this geomagnetic field for each X, Y, and Z component separately. Having the cosine coefficients as X_C^m and the sine coefficient as X_S^m and similarly for the Y and Z fields components, the intermediate coefficients $a_n^m, b_n^m, c_n^m\ and\ d_n^m$ are computed for m>0 using (Campbell, 1997):

$$a_n^m = \frac{2n+1}{4n(n+1)} \int_0^{180} \left[X_c^m \frac{dp_n^m}{d\theta} \sin\theta + Y_s^m m\, p_n^m\right] d\theta \tag{8}$$

$$b_n^m = \frac{2n+1}{4n(n+1)} \int_0^{180} \left[X_s^m \frac{dP_n^m}{d\theta} \sin\theta - Y_c^m m\, P_n^m\right] d\theta \tag{9}$$

$$C_n^m = \frac{2n+1}{4n(n+1)} \int_0^{180} Z_c^m\, P_n^m\ \sin\theta\, d\theta\,,$$
$$but\ if\ m = 0, C_n^o = 2C_n^m \tag{10}$$

$$d_n^m = \frac{2n+1}{4} \int_0^{180} Z_s^m\, P_n^m \sin\theta d\theta \tag{11}$$

The integral sign $\int$ found in Equations (8)-(11) means a summation over a θ which ranges from $0\ to\ 180°$; therefore, for computation we replaced the integral sign by summing over that range in finite increments of $\Delta\theta$ (2.5° for this study) steps. For this study, the size of these steps is selected to be appropriate to the wavelength resolution which is to be accomplished by the spherical harmonic analysis (SHA) fitting. We can then compute what will be the Legendre polynomial (Schmidt) coefficient from the values of Equations (8)-(11):

$$a_n^{me} = \frac{(n+1)a_n^m + c_n^m}{2n+1}\ ; \qquad a_n^{mi} = \frac{na_n^m - c_n^m}{2n+1} \tag{12}$$

$$b_n^{me} = \frac{(n+1)b_n^m + d_n^m}{2n+1}\ ; \qquad b_n^{mi} = \frac{nb_n^m - d_n^m}{2n+1} \tag{13}$$

where $a_n^{me} and\ b_n^{me}$ are the external cosine and sine spherical harmonic analysis (SHA) coefficients $a_n^{mi}\ and\ b_n^{mi}$ are the internal values.

Taking the real (z) and imaginary parts (-p) of the transfer function C_n^m which was devised by Schmucker (1970), generalized by Campbell and Anderssen (1983) and modified by Campbell (1989) as:

$$C_n^m = Z - iP \tag{14}$$

where

$$Z = \frac{R}{n(n+1)} \left\{ \frac{A_n^m[na_n^{me} - (n+1)a_n^{mi}] + B_n^m(nb_n^{me} - (n+1)b_n^{mi})}{(A_n^m)^2 + (B_n^m)^2} \right\} \tag{15}$$

and

$$P = \frac{R}{n(n+1)} \left\{ \frac{A_n^m[nb_n^{me} - (n+1)b_n^{mi}] - B_n^m(na_n^{me} - (n+1)a_n^{mi})}{(A_n^m)^2 + (B_n^m)^2} \right\} \tag{16}$$

Using R as the Earth radius in kilometers, Z and P are given in kilometers, and the coefficient summation are given by:

$$A_n^m = \left(a_n^{me} + a_n^{mi}\right) and\ B_n^m = \left(b_n^{me} + b_n^{mi}\right) \tag{17}$$

In each spherical harmonic analysis (SHA) coefficient of order m and degree n, the depth in kilometers to a conductivity layer (σ in s/m) which produces the measured observed field is given by Campbell (1997) as:

$$d_n^m = Z - P \tag{18}$$

Also, the substitute conductivity layer σ_n^m in Sm^{-1} is given as:

$$\sigma_n^m = \frac{5.4\ x\ 10^4}{m(\pi P)^2} \tag{19}$$

The ratio of the internal to external components of the surface geomagnetic field is then expressed as:

$$S_n^m = U - iV \tag{20}$$

where

$$U = \frac{(a_n^{me})(a_n^{mi}) + (b_n^{me})(b_n^{mi})}{(a_n^{me})^2 + (b_n^{me})^2} \tag{21}$$

and

$$V = \frac{(b_n^{me})(a_n^{mi}) + (a_n^{me})(b_n^{mi})}{(a_n^{me})^2 + (b_n^{me})^2} \tag{22}$$

The data analysis started by selecting first the five geomagnetically quietest days of each month from the 10 international quiet days (IQD) for the years under study for each of the regions used for the research.

This IQD indicate when the variations of the geomagnetic field are minimal for each month (Bolaji et al., 2013). Consequently, the five quietest days hourly values were added up hour by hour in each month and their mean value obtained. This therefore results to twenty-four hourly averages (means) for each month of the year (monthly average) for each of the geomagnetic components (H, D, and Z). This monthly mean facilitates elimination of the daily variability present in the procured data. The base line values of the geomagnetic components denoted as B are calculated using 2 h flanking the local midnight level (that is, between 24:00 and 01:00 LT) and it is written as;

$$B_0 = \frac{B_1 + B_2}{2} \quad (23)$$

where B_1 and B_2 are the horizontal (H), Declination (D) and vertical intensity (Z) hourly values at 24:00 and 01:00 LT hours. Also, the Sq amplitudes were obtained by taking the difference between the midnight baseline (B_0) values of a particular day and each of the hourly values of that same particular day. This is seen to be approximately equal to the hourly solar quiet (Sq) of each element and is expressed as;

$$dB = B_t - B_0 \quad (24)$$

where t = 1, 2……24 h. This was done so that at night in the absence of the sun the geomagnetic field starts from the same baseline value. The data analysis was done using the concept of local time (LT). Furthermore, the Fourier analysis was carried out on the monthly data of each geomagnetic (H, D and Z) components with the Fourier cosines and sine's coefficient truncated at order, m = 4. The Fourier series coefficient allows for the reconstruction of the Sq for the regions for each month of the year. This was followed by the polynomial fitting on the latitudinal variations of the regions field Fourier components and the computation of the Legendre polynomial (Schmidt) functions. Then we will calculate Lengendre polynomial (SHA) coefficients to order 4 and degree 12 (in order to eliminate errors and noise which took place at higher order and degree). The separation of the internal (induced) and an external (source) current in the study area was established using the output from the spherical harmonic analysis (SHA) analysis. Finally, the subsurface conductivity depth profile which could be responsible for the induced internal field observed was computed. Figure 1 shows the data processing flow chart.

RESULTS

The conductivity-depth profiles for Hartebeesthoek, Hermanus, Maputo and Tsumeb are presented in Figures 2, 3, 4 and 5 respectively. Figure 6 is the plot of the profiles on the same scale, showing only the fitted regression lines. This is done for clear understanding and comparison of the fluatuations found in the mantle conductivity depth profile along the study areas. The plots showed scattered points with high concentration from upper mantle down to approximately 800 km declining in density of the scatter at greater depths beyond 800 km depth. A number of factors could be attributed to the scatter which is observed in the plots among which are: variability of source current location, error from SHA fitting, error from field measurements and geomagnetic fields contributions that are produced by sources not from solar quiet time (Sq) field variations (such as lunar, etc). The trend of the conductivity depth structure in the study area is clearly supported; even though the scatter may indicate that some inflections in the regression fittings are poorly constrained. Therefore, what is determined as error is only but a measure of the regression fittings from the profile computed values distribution. In order to obtain mean values of the scattered conductivity-depth values, a polynomial trend line of order, $m = 3$ was fitted on the data points. This is based on a locally weighted profile regression fitting described by Cleveland (1979). Also, the software employed yielded detailed error analysis which is based on the standard deviations of the profile's conductivity values from the regression fittings. Hence from the profiles regression fittings, the error bars for Hartebeesthoek, Hermanus, Maputo and Tsumeb, represent the standard deviation of the conductivity values. The standard deviation values for Hartebeesthoek, Hermanus, Maputo and Tsumeb were correspondingly found to be 0.08097, 0.1001, 0.09227 and 0.05344 respectively.

The calculated average electrical conductivity values of Hartebeesthoek showed that the conductivity-depth profile commenced from 0.028 Sm^{-1} at 76.4 km depth and gradually increases to 0.070 Sm^{-1} at 105.8 km depth. It then decreased to 0.041 Sm^{-1} at 110.5 km. The conductivity values rose again from 0.053 Sm^{-1} at a depth of 110.8 km and decreases again to 0.036 Sm^{-1} at a depth of 111.4 km. It continued to fluctuate with a very sharp increase in conductivity until it attained 0.139 Sm^{-1} at 227.8 km, 0.187 Sm^{-1} at 375.0 km, 0.193 Sm^{-1} at 415.0 km and 0.269 Sm^{-1} at 665.5 km. At 711.2 km depth, the conductivity recorded was 0.280 and 0.340 Sm^{-1} at 874.5 km depth. Finally, the conductivity-depth profile continued to rise in the upper mantle until it attained a peak value of 0.498 Sm^{-1} at a depth of 1052.8 km exhibiting no indication of leveling off at the lower mantle. On the other hand, the result from Hermanus region showed that the electrical conductivity-depth profile started from about 0.039 Sm^{-1} at about 84.0 km depth and rose gradually to about 0.050 Sm^{-1} at 123.84 km and 0.118 Sm^{-1} at 235.6 km depth. Then the profile increased steadily untill it attained 0.142 Sm^{-1} at 378.3 km, 0.145 Sm^{-1} at 440.8 km, 0.218 Sm^{-1} at 661.8 km and 0.239 Sm^{-1} at 759.4 km. It then attained a value of 0.279 Sm^{-1} at 877.4 km depth and a highest value of 0.323 Sm^{-1} at 1467.0 km depth.
Furthermore the conductivity-depth profile of Maputo started with 0.057 Sm^{-1} at about 141.0 km depth and increased rapidly to about 0.154 Sm^{-1} at 183.5 km depth upto 0.231 Sm^{-1} at 285.9 km. The profile continued to increase until it reached 0.195 Sm^{-1} at 359.0 km, 0.225 Sm^{-1} at 405.9 km, 0.318 Sm^{-1} at 667.0 km, 0.347 Sm^{-1} at 807.0 km and 0.387 Sm^{-1} at 1160.8 km depth as its maximum depth. The Tsumeb conductivity-depth profile commenced with 0.025 Sm^{-1} at a depth of about 112.0 km and rises rapidly to about 0.059 Sm^{-1} at 237.1 km depth. The profile then rises again to 0.081 Sm^{-1} at 371.7 km depth; it then continued fluctuating until it reached 0.126 Sm^{-1} at 625.3 km depth. There were no conductivity values between 673.9 km till 1065.8 km depth from where the profile started rising rapidly until it reached its maximum value of 0.187 Sm^{-1} at 1289.5 km depth which was also the maximum depth of penetration within the region.

DISCUSSION

The mantle conductivity depth profiles of the Southern African regions show generally an increase in conductivity

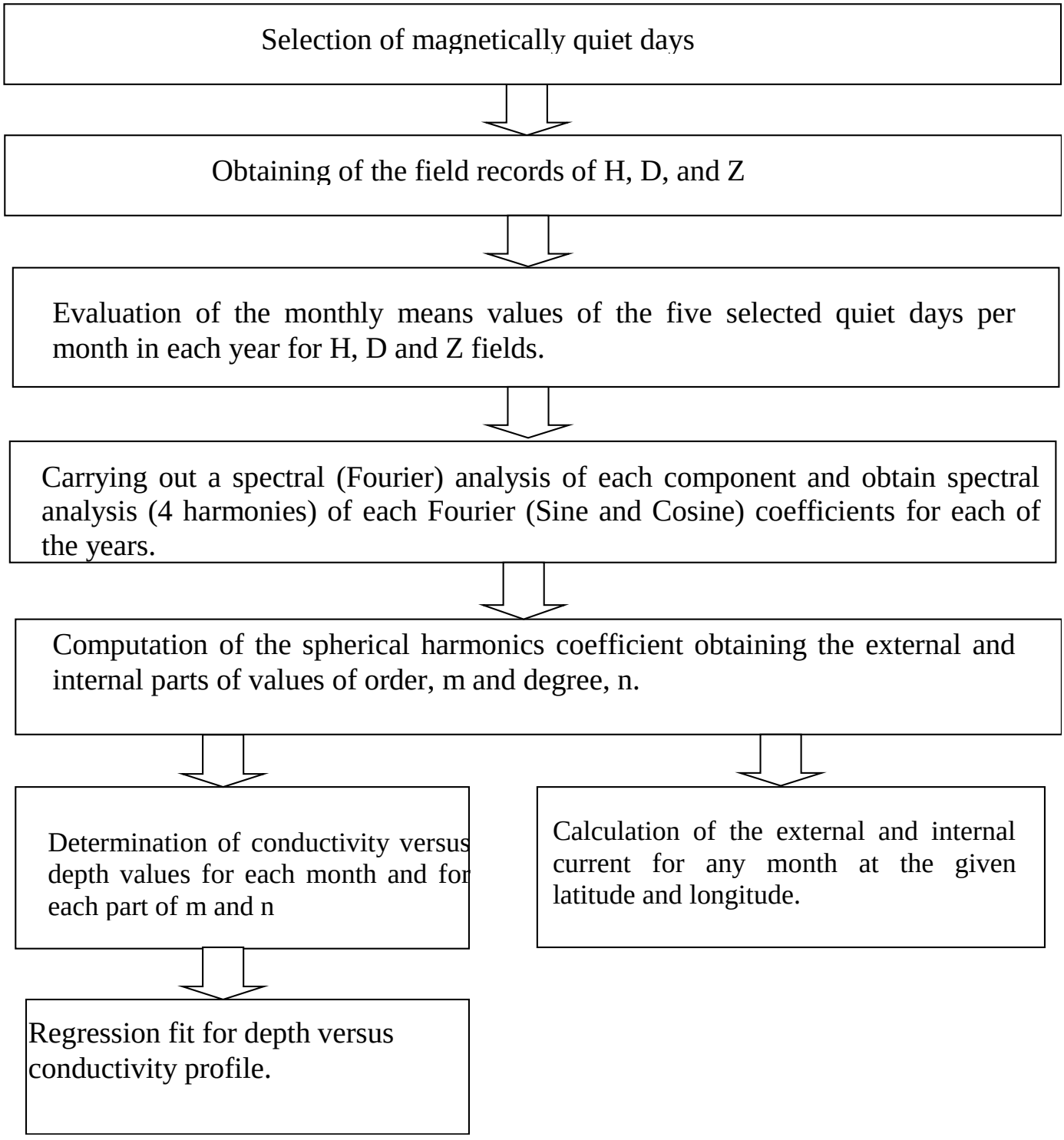

Figure 1. Data processing flow chart.

from the crust down to the mantle apart from some areas where discontinuities in earth layers were seen. This is thus found to be in agreement with global model that showed a steep increase in the conductivity profile from about 300 - 700 km. (Abidin et al., 2019; Ugbor et al., 2016; Obiora et al., 2015; Obiekezie and Okeke, 2010; Neal et al., 2000; Campbell et al., 1998; Arora et al., 1995; Campbell and Schiffmacher, 1987; Didwall, 1984). At the maximum penetration depths of 1052.8, 1467.0, 1160.8 and 1289.5 km in Hartebeesthoek, Hermanus,

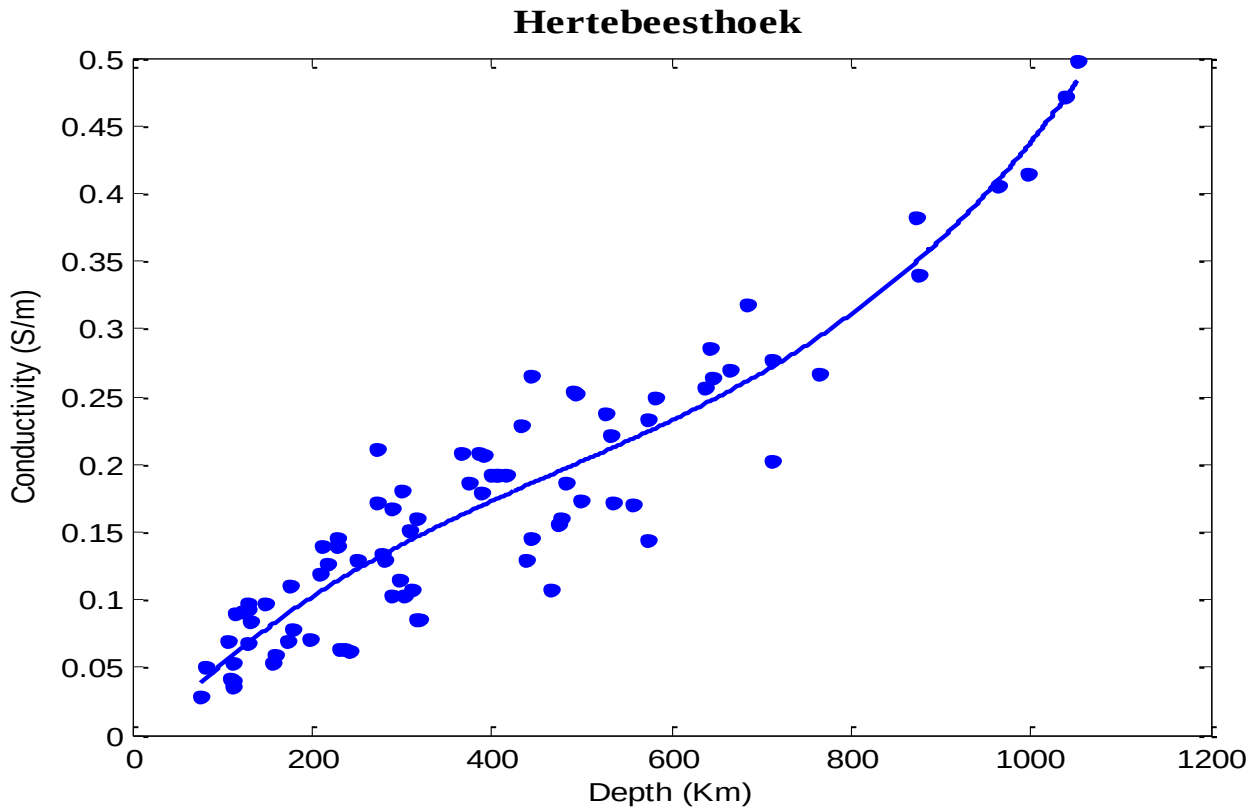

Figure 2. Mantle electrical conductivity-depth profile of Hartebeesthoek.

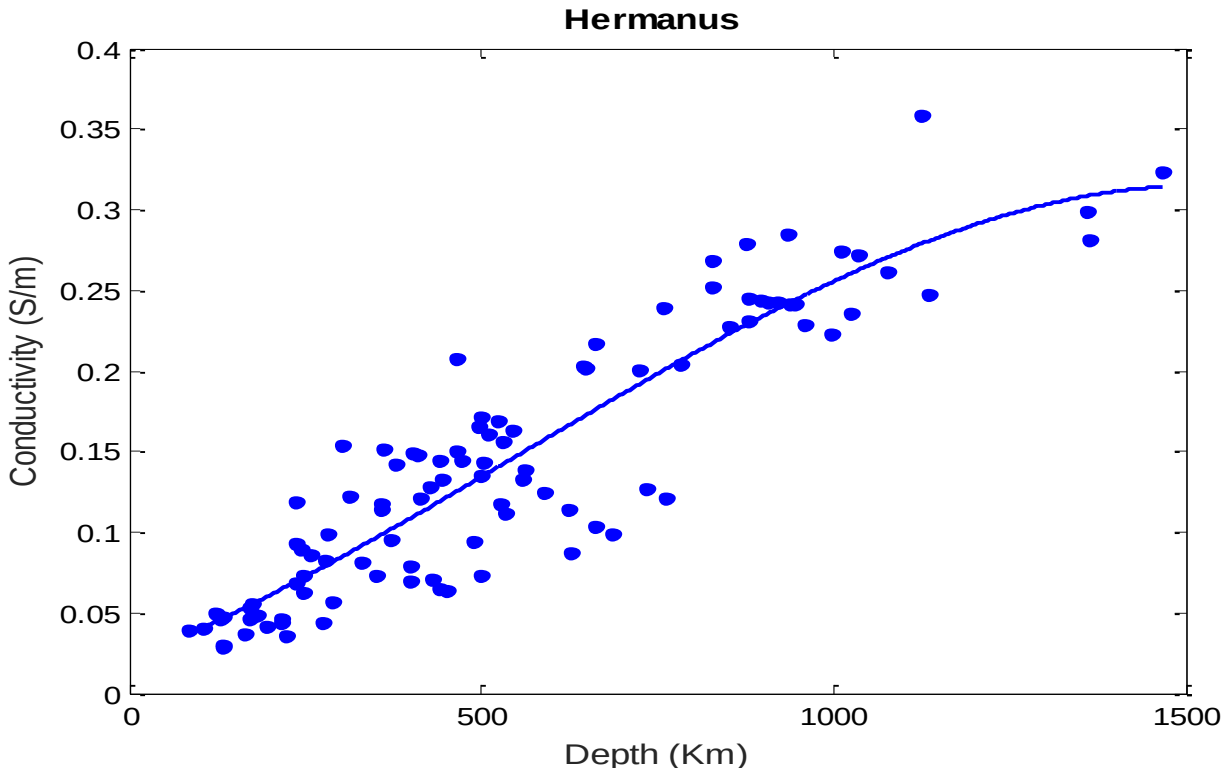

Figure 3. Mantle electrical conductivity-depth profile of Hermanus.

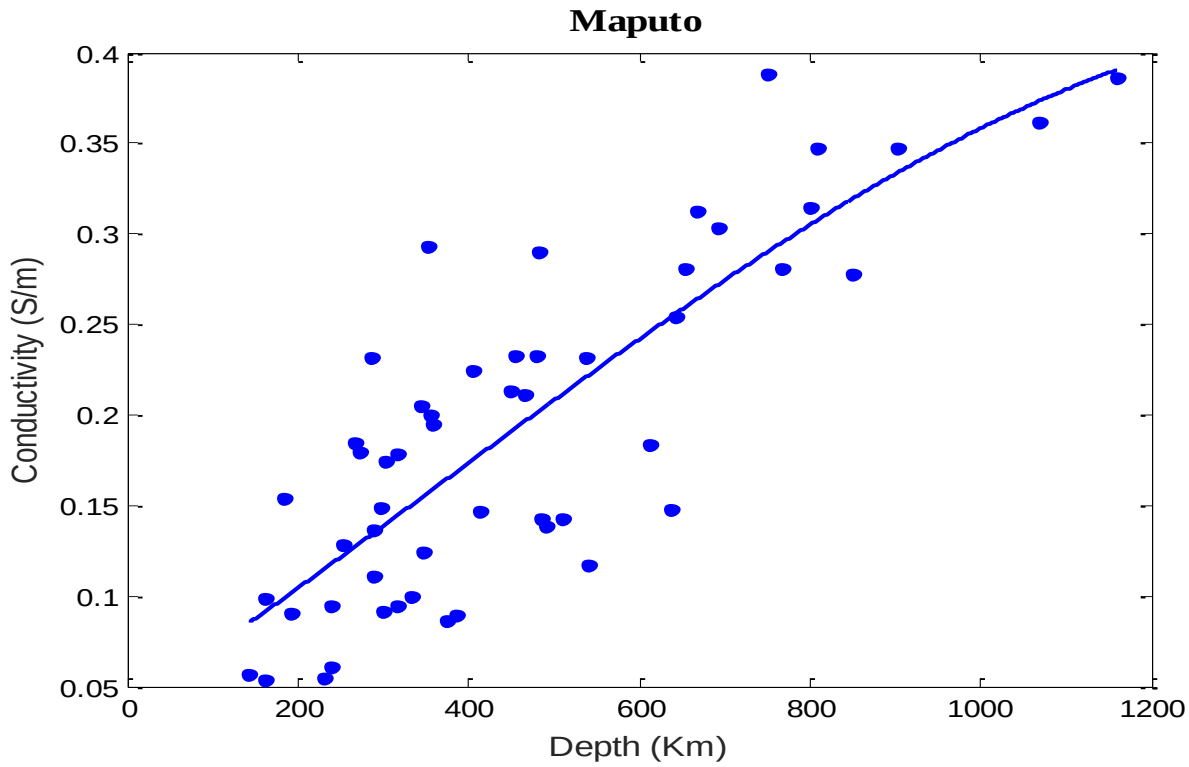

Figure 4. Mantle electrical conductivity-depth profile of Maputo.

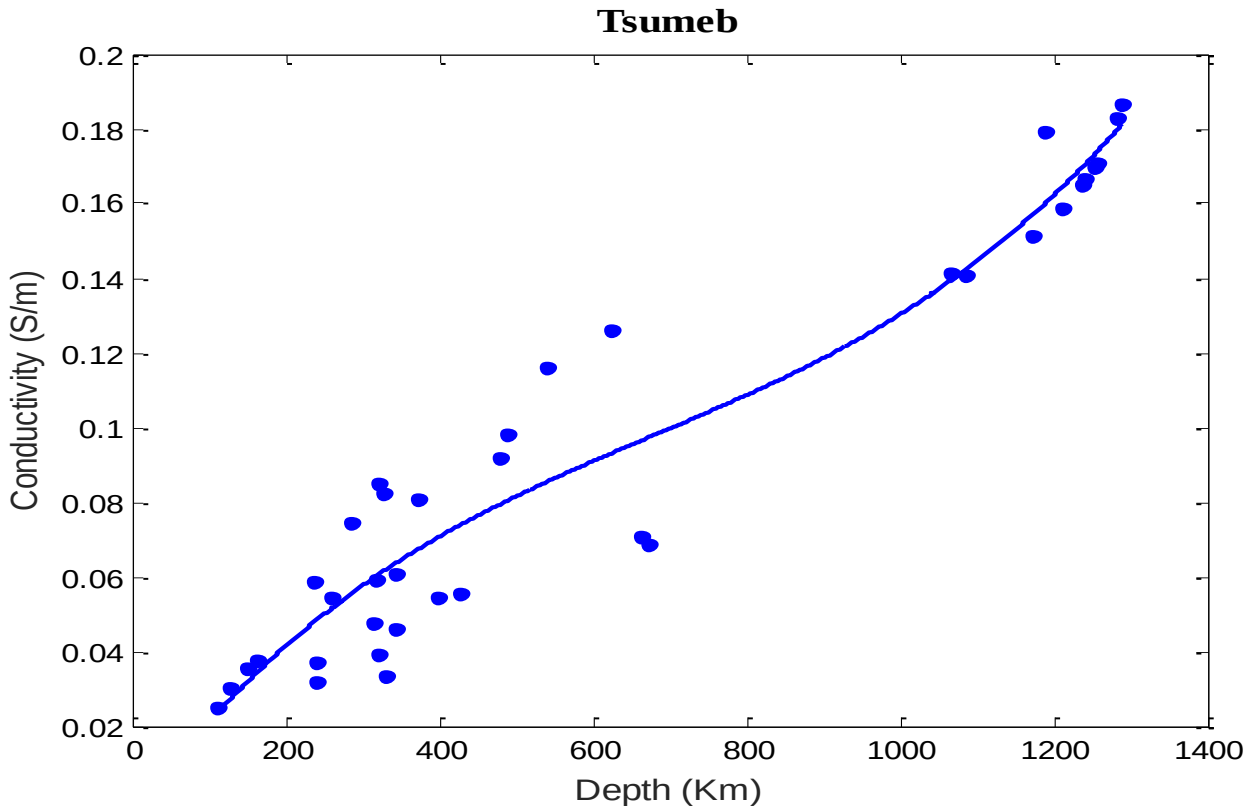

Figure 5. Mantle electrical conductivity-depth profile of Tsumeb.

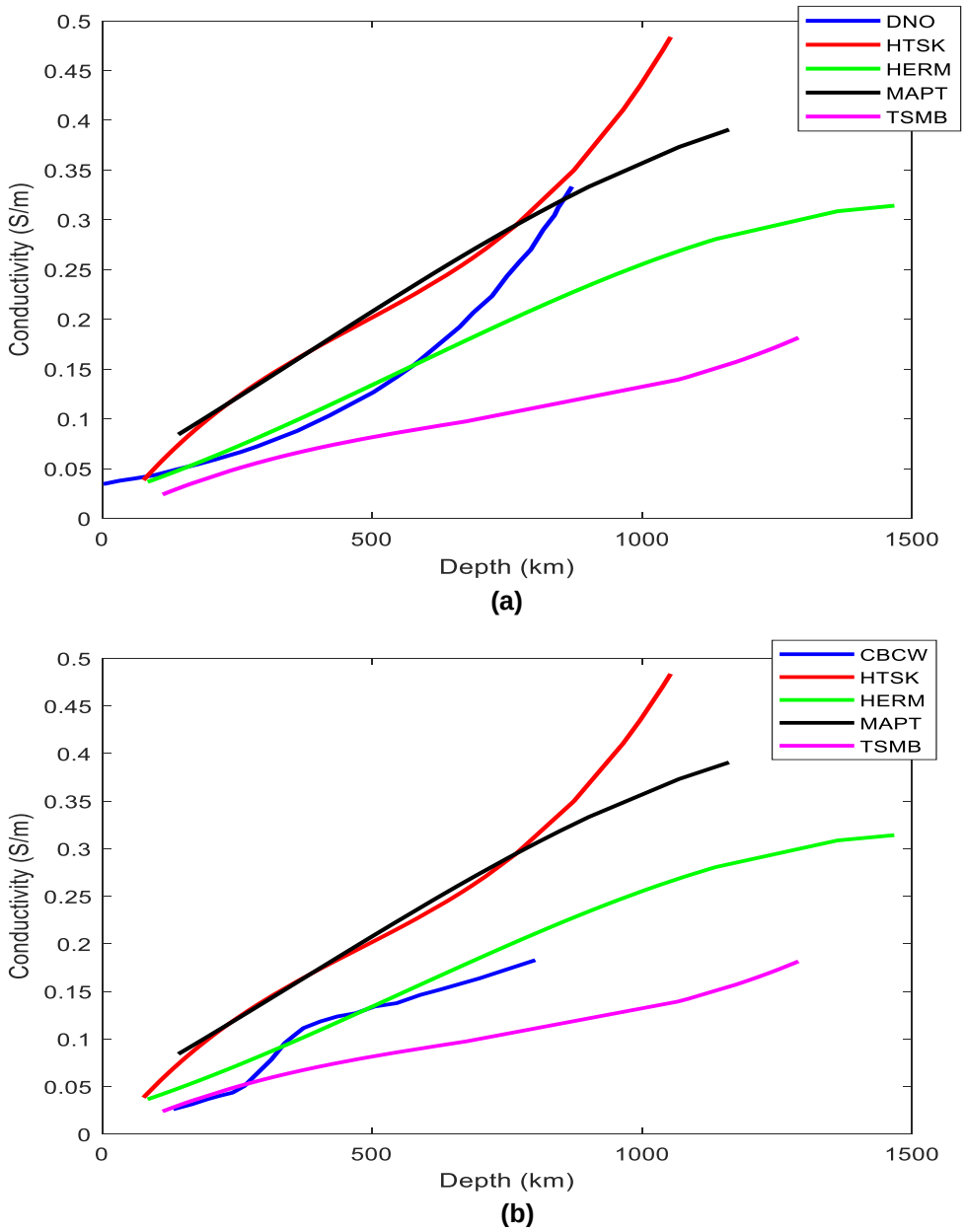

Figure 6. Present profiles (HTSK, HERM, MAPT, and TSMB) compared with: (a) DNO: Obiora and Okeke (2013); and (b) CBCW: Campbell and Schiffmacher (1988).

Maputo and Tsumeb, the calculated conductivity reached the greatest values of 0.498, 0.323, 0.387 and 0.187 Sm^{-1}, respectively. From these results, Hermanus, Tsumeb and Maputo are observed to have greater depth of Sq penetration than Hartebeesthoek; this may be attributed to the composition of mantle in that area and oceanic effect since they all lie along the coastal region. Also, all the profiles have similar trend lines even though some are more similar to each other; exhibiting steep slopes between the crust and the depth of about 400 km.

Moreover, in Hartebeesthoek, Hermanus, Maputo and Tsumeb, the average electrical conductivity values calculated are 0.028, 0.039, 0.057 and 0.0.025 Sm^{-1} at depths of 76.4, 84.1, 141.0 and 111.6 km respectively. These values rose to a certain value of 0.228, 0.207, 0.205 and 0.116 Sm^{-1} at depths of 433.6, 465.3, 345.4 and 541.6 km respectively. This increase in conductivity at the crust and some parts of the upper mantle within the first few kilometers agrees closely with works of Campbell and Schiffmacher (1988) who argued that the temperature of the Earth increases with depth, so, the electrical conductivity increases with depth since it depends on temperature. Also, the high conductivity values seen in the crust were explained by Obiora and Okeke (2013) to

be caused by: (i) the presence of conductive graphite which is associated with the extensive shear zones within the Precambrian basement (Gough, 1983) and (ii) the hydrated conductive oceanic materials incorporated into the continental crust (Drury, 1978).

Consequently, the electrical conductivity profile of this study showed that the conductivity values increased between 110.0 and 320.0 km depths corresponding to the region of global low velocity seismic zone with high conductivity (Tarits, 1994; Kennett and Engdahl, 1991; Dziewonski and Anderson, 1981). Obiora et al. (2015) and Campbell and Schiffmacher (1988) also observed similar increase in conductivity between 150.0 and 350.0 km in East Asia and African sector respectively. This conductivity increase within the low velocity seismic zone is attributed to the presence of partial melting (Thybo, 2006). Sequentially, the conductivity depth profiles of Hartebeesthoek and Tsumeb have similar trend lines but differ slightly from Hermanus and Maputo (which are also similar) showing a sharp increase in electrical conductivity before 420.0 km depth. This region is found to be within the mantle transition zone of the Earth; between the lower mantle as well as the upper mantle at 400 and 670 km depths. The estimated conductivity of Hartebeesthoek and Tsumeb profile declined substantially between the depth range of 420.0 and 480.0 km with a sharp steep rise thereafter. Besides this sharp rise, an evidence of discontinuities was also observed in the two profiles. These discontinuities result due to olivine atoms rearrangement (constituting mainly peridotite) forming a high dense crystal structure at 400.0 km depth, as a result of pressure increase with increasing depth. This is because the primary composition of the Earth's mantle, including the transition zone is peridotite, which is an ultramafic igneous rock. Also, evidence shows that at depth below 670.0 km, atoms yet rearrange again to form an even higher denser crystal structure. This increase in conductivity within this region is attributed to the 410.0 km seismic discontinuity (Arora et al., 1995). At the depths of 128.0 and 317.0 km, the conductivity values of Hartebeesthoek and Tsumeb are 0.097 and 0.160 Sm^{-1} and 0.030 and 0.059 Sm^{-1}, respectively. Beyond 1000.0 km depth, both profiles showed an increase in conductivity within the lower mantle with no indication of leveling off. Findings from this work supported the assertion made by Campbell and Schiffmacher (1988) that beneath Asia and Africa, the upper mantle below 400.0 km depth is highly conductive.

On the other hand, Hermanus and Maputo profiles obtained showed different trends lines to that of the other two regions showing gradual increase in the electrical conductivity especially from the uppermost part of the upper mantle (lithosphere) to 800.0 km depth within the lower mantle. An evidence of discontinuities were also observed near 410.0 –580.0 km, 580.0 - 880.0 km and 1136.0 km for Hermanus stations and 200.0 – 300.0 km, 350.0 - 680.0 km and 680.0 - 1160.0 km for Maputo stations. These locations structurally are also within the transition zone. Roberts (1986) projected that the contrast found in conductivity at 500.0 - 1000.0 km depth range could be attributed to the 670 km seismic discontinuities. From here, conductivity increases rapidly and significantly with depth as observed in our study. The mantle transition zone is established to be the most important water reservoir on Earth because it has the capability of accommodating water content (Ohtani and Sakai, 2008). In recent years, geophysical explorations e.g. electrical conductivity is observed to be sensitive to water content (Wang et al., 2006). Therefore the presence of water may influence the enhanced conductivity values found in the transition zones. Also at depths of 332.0, 359.0 and 414.0 km, the conductivity values in Hermanus and Maputo are 0.082, 0.114, 0.121 and 0.100, 0.195, 0.146 Sm^{-1} respectively. Beyond 850.0 km, both profiles suddenly increased in conductivity within the lower mantle.

It is observed from this study that two most conductive Earth layers exist within the Southern African regions. These are found at about 100.0 to 400.0 km in the upper mantle and beyond 850.0 km within the lower mantle. This two layers agree with: (i) Onwumechili and Ogbuehi (1967) who showed that the depth of perfectly conducting layer in Nigeria to be exactly at 200.0 km; (ii) Chandrasekhar (2011) who calculated that the average depth of a substitute conductor beneath the India region is about 1200.0 km. Slight fluctuations in the conductivity profile are observed at about 400.0 to 1000.0 km depths and is attributed to the changes in phase of olivine atoms (which is the chief constituent of mantle rocks) at greater depths. This change in phase results due to an increased pressure and temperature at such great depths (Katsura and Ito, 1989).

There are some similarities in the four profiles plotted in Figure 6. All have conductivities below 0.100 Sm^{-1} at the shallower depths. Most given evidence of an increase in electrical conductivity are observed after about 250 km, whereas Tsumeb has conductivities below 0.100 Sm^{-1} at the shallower depths to about 673.9 km depth and show evidence of an increase in electrical conductivity from about 1065.8 km. This agrees well with global model that showed a steep increase in electrical conductivity. Apparent discontinuities are found in the conductivity profiles in all but it is more prominent in Tsumeb profile. In all, HTSK has the highest conductivity values and TSMB the least. There is greatest Sq penetration in HTSK, followed by TSMB. At more than 400.0 km depth, HTSK, MAPT and HERM have the highest values of conductivity and TSMB as the least. The electrical conductivity result from Tsumeb profile was smaller than the Harteesthoeck profile which has very high values starting from 0.110 Sm^{-1} at 176.3 km to 0.498 Sm^{-1} at depth of 1052.8 km, whereas Tsumeb profile high values started from 0.116 Sm^{-1} at 541.6 km to 0.187 Sm^{-1} at 1289.5 km with the deepest penetration depth. This

portrays that the mantle electrical conductivity that depends mainly upon the chemical composition, saturation phase, rock type and prevailing temperature are different among the continents as also concluded by Glover and Vine (1994).

The Sq current depth of penetration is least in Maputo which is 1160.8 km with conductivity of 0.387 Sm^{-1} while Hermanus has the highest depth of Sq current penetration of 1467.0 km with conductivity of 0.323 Sm^{-1}. Maputo has generally higher conductivity values than Hermanus station; and in all, Harteesthoeck has the highest conductivity values with respect to the depth whereas Tsumeb has the least. This difference in the trend line of the profiles may be attributed to the differences in the geology of the areas. Law and Riddihough (1971) suggested that the geological features of an environment should be associated with the conductivity anomalies in that environment. For instance, Mozambique formations are underlain primarily by extremely old Precambrian metamorphic and igneous crystalline basement rock, mainly greenstone belts and granite-gneisses (Schluter, 2006). South African region composed of Precambrian crystalline rocks, mainly gneisses, granites, metasediments, and volcanic sequences (metavolcanic rocks) generally referred to as greenstone belts. The Tsumeb region is underlain within a thick sequence of Precambrian polymetallic carbonate rocks. The conductivity profiles of Hermanus and Maputo have similar trends with no intersection at any depth. The non-intersection at any depth of these two profiles is an indication of lateral variations that exist between the continental mantle which may be due to large scale convective heat flow pattern beneath the continent region which has been earlier identified on seismology records by Anderson and Dziewonski (1984).

Hartebeesthoek and Maputo profile showed strong agreement at about 200.0 - 480.0 km and 750.0 – 800.0 km depth range with evaluated average values of electrical conductivity of 0.100 - 0.180 Sm^{-1} and 0.290 Sm^{-1} respectively. This suggests similarities in the geological composition of the areas at these depths. We therefore suggest that about 200.0 – 480.0 km and 750.0 – 800.0 km depth range are likely to be areas where the chemical compositions of the Earth are homogeneous and the materials in the area are subjected to nearly the same conditions of pressure and temperature. Interestingly, Hartebeesthoek and Maputo are found to be closer to each other and they are on the eastern part of Southern African region. Meanwhile, Hermanus and Tsumeb profiles showed no intersection with any of the other profiles. The non-intersection depicts lateral differences between the regions under study. This is not surprising; Tsumeb region is located in the western part while Hermanus is found in the southern part of the study region, all within Southern African region.

The results of the conductivity-depth profiles of the present study show similar trends and compares well with previous researches done in different regions of the globe (Obiora and Okeke, 2013; Campbell and Schiffmacher, 1988) as illustrated in Figure 6. For instance, the results of the present study in Southern African region are compared with the results of Obiora and Okeke (2013), in West African sector (blue trend line) that is located on equatorial region. As can be seen from Figure 6a, at depth of about 90.0 and 850.0 km, and 150.0 and 580.0 km, the present profiles of Maputo and Hermanus agrees closely with the West African conductivity-depth profile respectively. This likely suggests that the same geological conditions in the Earth's interior bound the sub-continental layers. The West African profile which started at shallowest depth of about 2.0 km has the least penetration depth of 860.0 km when compared with the present study, showing also large lateral variation with Tsumeb profile. On the other hand, the work of Campbell and Schiffmacher (1988) in Australian region shown in Figure 6b though did not penetrate deeper into the Earth as our work in Southern African region, but they compare very well. However, there is no evidence of the Campbell and Schiffmacher (1988) conductivity profile having the same values at any depth with Hartebeesthoek and Maputo profiles. This we suggest may depict lateral differences between these areas with our results being consistently higher. Also in Figure 6b, at depth range of about 110 - 200 km and 480.0 - 520.0 km, Campbell and Schiffmacher (1988) conductivity-depth profile is observed to closely agree with the Tsumeb and Hermanus profile. We therefore suggest that about 110.0 - 200.0 km and 480.0 - 520.0 km depth range may be regions within the earth’s mantle where the chemical compositions of the interior of the Earth are homogeneous and the substances there are subjected to nearly similar conditions of pressure and temperature. The intersections that exist between our profiles and that of Obiora and Okeke (2013) and Campbell and Schiffmacher (1988) within some sections of the upper mantle are found to be in agreement with global model which is obtained on the assumption of a spherical homogeneous Earth (Banks, 1972). The intersection around the 410.0 discontinuity is very prominent in Figure 6b. Campbell and Schiffmacher (1988) also observed the 410.0 km discontinuity which we also observed in our profiles. Their electrical conductivity value at 133 km depth was 0.024 Sm^{-1} which rapidly rose to 0.053 Sm^{-1} at 278.0 km depth, rising continuously through 0.118 Sm^{-1} at the 410.0 km depth to 0.184 Sm^{-1} at 807.0 km depth.

From Figures 2 to 6, some outstanding features were revealed after careful observation of the electrical conductivity profiles. The penetration depth of about 1467.0 km obtained of solar quiet day (Sq) current into the interior of the Earth is greater than those obtained by other researchers in the African regions. This may be attributed to the effects from the deeper 3-D structures, the hydrated transition zone and effect from the ocean.

Also, highest electrical conductivity value of 0.498 Sm^{-1}

obtained is more than those of the previous researchers. This feature may be attributed to greater solar zenith angle within the local summer hemisphere which initiated the higher electrical conductivity (Yamazaki et al., 2012c). The enhanced electrical conductivity within the ionosphere could have been inducted into the Earth's interior with the consequential effect of increasing the Earth's conductivity. Electrical conductivity of the Earth depends on the mobility and the amount of free particle charges. Although, Campbell and Schiffmacher (1985, 1988), Takeda (2002), Chen et al. (2008), El Hawary et al. (2012), and Bolaji et al. (2015) have investigated hemispheric variability of Sq currents over Africa, America, and Asia sectors, they suggested that southward Sq focus in the Southern Hemisphere is characterized by westward currents in the daytime (Bolaji et al., 2015). We noted also that punctuated discontinuities exists in the Earth's electrical conductivity as was equally observed in all the profiles of this study but more pronounced in Tsumeb region at depths of about 673 - 1065 km.

From these result, we are therefore proposing that not only EEJ contributes to the greater depth of Sq current penetration but also the effects from the deeper 3-D structures, the hydrated transition zone and effect from the ocean. This is because we obtained greatest depth of Sq current penetration in the Southern African region which is very far from the geomagnetic equator.

Conclusion

This work has successfully obtained the electrical conductivity depth profiles of the upper mantle in the Southern African regions from the estimation of Fourier coefficients and evaluation of spherical harmonics coefficients on the geomagnetic field components. The usefulness of this work is that these profiles will improve understanding of Sq current variations in mapping mantle conductivity. The variations of the Sq current found in the geomagnetic data of Hartebeesthoek, Hermanus, Maputo and Tsumeb were used to profile the Earth conductivity depth structure around the Southern African regions down to a depth of about 1467.02 km. Results obtained were compared to results of previous research works done in African region and other parts of the globe. We therefore draw the following conclusions: There is a downward increase in electrical conductivity within the Earth's interior which attains its maximum values within the lower mantle thereby agreeing with the global models. The interior of the Earth may be viewed as a stack of non-homogeneous materials as evidenced in the seismic wave model, with each layer, conductivity corresponding to the chemical and physical properties of the constituent materials. Southern African regions have the greatest Sq current depth penetration into the interior of the Earth than the previous researches carried out around the world. The calculated average conductivity values in the Southern African regions are evidently greater than those obtained in other parts of African regions. The results of our work although show higher conductivity values but the trend generally are consistent with the previous research works in Africa, which generally show the mantle layer as being highly conductive. There are evidences of discontinuities in the Earth layers and the profile's regression fit are seen to intersect at some points inside the Earth interior. We therefore contributed to knowledge by integrating the upper atmosphere and solid Earth's interior to determine conductivity-depth structure of Hartebeesthoek and Maputo regions. We are recommending that a chain of geomagnetic observatories be established around the world as a whole. Also, there should be a continuous and uninterrupted data acquired and fully analyzed to give us a better and comprehensive view of the nature of the Earth's interior.

CONFLICT OF INTERESTS

The authors have not declared any conflict of interests.

ACKNOWLEDGEMENTS

The authors are grateful to Prof. K. Yumoto of MAGDAS, Japan, for the data used in this work and Dr. Dan Okoh of Centre for Basic Space Science, Abuja, Nigeria for his valuable contributions.

REFERENCES

Abidin ZZ, Jusoh MH, Abbas M, Yoshikawa A (2019). Application of solar quiet (Sq) current in determining mantle conductivity-depth structure in Malaysia. Journal of African Earth Sciences 192:104776.

Agha SO, Okeke FN (2007). Estimation of the conductivity-depth ratio of the various sub-regions of the upper mantle using Sq current. The Nigerian Journal of Space 3:57-67.

Anderson DL, Dziewonski AM (1984). Seismic tomography. Scientific American 251(4):60-71.

Arora BR, Campbell WH, Schiffmacher ER (1995). Upper Mantle Electrical Conductivity in the Himalayan Region. Journal of Geomagnetism and Geoelectricity 47(7):653-665.

Banks RJ (1972). The overall conductivity distribution of the Earth. Journal of Geomagnetism and Geoelectricity 24(3): 337-351.

Bolaji O, Adimula I, Adeniyi J, Yumoto K (2015). Variability of horizontal magnetic field intensity over Nigeria during low solar activity. Earth Moon Planets 110(1-2):91-103.

Campbell WH, Anderssen RS (1983). Conductivity of the subcontinental upper mantle: an analysis using quiet- day records of North America. Journal of Geomagnetism and Geoelectricity 35(10):367-382.

Campbell WH, Schiffmacher ER (1985). Quiet ionospheric currents of the northern hemisphere derived from Geomagnetic field records. Journal of Geophysical Research 90: 6475–6486

Campbell WH, Schiffmacher ER (1986). Quiet ionospheric currents of the Northern Hemisphere derived from geomagnetic field records. Journal of **Geophysics** 90: 6475-6486.

Campbell WH, Schiffmacher ER (1988). Quiet ionospheric currents of the Southern Hemisphere derived from geomagnetic records. Journal of Geophysical Research: Space Physics 93(A2):933-944.

Campbell WH, Schiffmacher ER (1988b). Upper mantle electrical conductivity for seven subcontinental regions of the Earth. Journal of Geomagnetism and Geoelectricity 40(11):1387-1406.
Campbell WH (1987). The upper mantle conductivity analysis method using observatory records of the geomagnetic field. Pure and Applied Geophysics 125(2):427-457.
Campbell WH (1997). Introduction to geomagnetic fields. Cambridge University Press, New York.
Campbell WH (2003). Introduction to geomagnetic fields. Cambridge University Press, New York.
Campbell WH, Barton CE, Chamalaun FH, Welsh W (1998). Quiet-day ionospheric currents and their application to upper mantle conductivity in Australia. Earth Planet Space 50(4):347-360.
Canton J (1759). An attempt to account for the regular diurnal variation of the horizontal magnetic needle. Philosophical Transactions of the Royal Society of London 49:398-445.
Chapman S (1919). The solar and lunar diurnal variation of the Earth's magnetism. Philosophical Transactions of the Royal Society of London 218(561-569):1-118.
Chapman S, Price A (1930). The electric and magnetic state of the interior of the Earth, as inferred from terrestrial magnetic variations. Philosophical Transactions of the Royal Society of London 229(670-680):427-460.
Chandrasekhar E (2011) "Regional Electromagnetic Induction Studies Using Long Period Geomagnetic Variations". Chapter 3, in The Earth's Magnetic Interior, Vol. 1, edited by E. Petrovský, E. Herrero-Bervera, T, Harinarayana and D. Ivers, pp. 31 – 42, Springer Dordrecht Heidelberg London New, York.
Chen CH, Liu JY, Yumoto K, Lin C H, Fang TW (2008). Equatorial ionization anomaly of total electron content and equatorial electrojet in ground-based geomagnetic field strength. The Journal of Atmospheric and Solar-Terrestrial Physics 70(17):2172-2183.
Cleveland WS (1979). Robust locally weighted regression and smoothing scatter plots. American Statistical Association 74(368):829-836.
Didwall EM (1984). The electrical conductivity of the upper mantle as estimated from satellite magnetic field data. Journal of Geophysics Research 89(B1):537–542.
Drury MJ (1978). Partial melt in the asthenosphere: evidence from electrical conductivity data. Physics of the Earth and Planetary Interiors. 17(2):P16-P20.
Dziewonski AM, Anderson DL (1981). Preliminary reference Earth model. Physics of the Earth and Planetary 25(4):297-356.
Hawary RE, Yumoto K, Yamazaki Y, Mahrous A, Ghamry E, Badi K, Meloni A, Kianji G, Uiso CBS, Mwiinga N, Joao L, Affluo T, sutcliffe PR, Mengistu G, Baki P, Abe S, Ikeda A, Ikeda A, Fujimoto A, Tokunaga T (2012). Annual and semi-annual Sq variations at 960 MM MAGDAS I and II stations in Africa. Earth Planets Space 64(6):425-432.
Gauss CF (1838). Allgemeine Theories des Erdmagnetismus, in Resultate aus den Beobachtungen des magnetischem Vereins in Yahr, edited by C. F. Gauss and W. Weber: translated from the German by E. Sabine and R. Taylor. Sci. Mem. Select. Trans. For. Acad. Learned Soc. Foreign J. 2:184 -251, 1841.
Gauss CF (1939). Allgemeine Theories des Erdmagnetismus 1. https://link.springer.com/chapter/10.1007/978-3-642-49319-5_5
Gough DI (1983). Electromagnetic geophysics and global tectonics. Journal of Geophysical Research: Solid Earth, 88(B4):3367-3377.
Glaßmeier KH, Soffel H, Negendank J (2009). Geomagnetic Field Variations, Advances in Geophysical and Environmental Mechanics and Mathematics. Springer-Verlag Berlin Heidelberg.
Glover PW, Vine F (1994). Electrical conductivity of the continental crust. Geophys. Research Letters. 21(22):2357-2360.
Graham G (1724). An account of the observations made of the variation of the horizontal needle in London in the later part of the year 1722 and beginning of 1723. Philosophical Transactions of the Royal Society of London A32:96-107.
Katsura T, Ito E (1989). The system Mg2SiO4 _ Fe2SiO4 at high pressures and temperatures: precise determination of stabilities of olivine, modified spinel and spinel. Journal of Geophysical Research 94(B11):15663-15670.
Kennett B, Engdahl E (1991). Travel times for global Earthquake location and phase identification. Geophysical Journal International. 105(2):429-465.
Kono M (2009). Geomagnetism Treatise on Geophysics. Elsevier Journal 5:1:30.
Langel RA (1982). Results from the magsat mission. Issue of the Johns Hopkins APL Technical Digest 3:307-324.
Law LK, Riddihough RP (1971). A geographical relation between geomagnetic variations anomalies and tectonics. Journal of Earth Science 8(9):1094-1106
Maxwell JC (1873). Treatise on Electricity and Magnetism. Cambridge University Press, London.
Neal SL, Mackie RL, Larsen JC, Schultz A (2000). Variations in the electrical conductivity of the upper mantle beneath North America and the Pacific Ocean. Journal of Geophysical Research 105(B4):8229-8242.
Obiekezie TN, Okeke FN (2010). Upper Mantle Conductivity Determined from the Solar Quiet Day Ionospheric Currents in the Dip Equatorial Latitudes of West Africa. Moldavian Journal of Physical Sciences 9(2):199-204.
Obiora DN, Okeke FN (2013). Crustal and upper mantle electrical conductivity structure in North Central Nigeria. International Journal of Physical Sciences 8(42):1975-1982.
Obiora DN, Okeke FN, Yumoto K (2015). Electrical conductivity of mantle in the North Central region of Nigeria. Journal of Earth System Science 101:274-281.
Ohtani E, Sakai T (2008). Recent advances in the study of mantle phase transitions. Physics of the Earth and Planetary 170:240-247.
Olsen N (1999). Induction studies with satellite data. Surveys in Geophysics 20:309-340.
Onwumechili CA, Ogbuehi PO (1967). Analysis of the magnetic field of the equatorial electrojet. Journal of Atmospheric and Terrestrial Physics 29(5):553-566.
Roberts G (1986). Global electromagnetic induction. Surveys in Geophysics 8(3):339-374.
Sabine E (1846). Contributions to Terrestrial Magnetism. No.VII. Philosophical Transactions of the Royal Society of London. 136(240):237-336.
Schluter T (2006). Geological Atlas of Africa. Springer pp. 180-183.
Schmucker U (1970). An introduction to induction anomalies. Journal of Geomagnetism and Geoelectricity 2:9-33.
Schuster A (1908). The diurnal variation of terrestrial magnetism. Philosophical Transactions of the Royal Society A 208:163-204.
Schuster A (1889). The diurnal variation of terrestrial magnetism. Philosophical Transactions London A180:467-518.
Tachard G (1688). A relation of the voyage to Siam: performed by six Jesuits sent by the French king, to the Indies and China in the year 1685.Wikipedia, the free encyclopedia.
Takeda M (2002). The correlation between the variation in ionospheric conductivity and that of the geomagnetic sq field. Journal of Atmospheric and Solar-Terrestrial Physics 64(15):1617-1621.
Tarits P (1994). Electromagnetic studies of global geodynamic processes. Surveys in Geophysics 15(2):209-238.
Thybo H (2006). The heterogeneous upper mantle low velocity zone. Tectonophysics 416(1-4):53-79.
Ugbor DO, Okeke FN, Yumoto K (2016). Mapping the earth conductivity-depth structure of African geomagnetic equatorial anomaly regions using solar quiet current variations. Journal of African Earth Sciences 116: 81-88.
Von Humboldt A (1863). Cosmos. Vol. V. English translation by E. C. Otte and W. S. Dallas. Harper and Bros. Pub., New York.
Wang D, Mookherjee M, Xu Y, Karato SI (2006). The effect of water on the electrical conductivity of olivine. Nature 443: 977.
Yamazaki, Y, Richmond AD, Liu HL, Yumoto K, Tanaka Y (2012c). Sq current system during stratospheric sudden warming events in 2006 and 2009. Journal of Geophysical Research 117: A12313.